ACTIVE VIBRATION CONTROL OF A SMART PLATE

Yavuz Yaman
Department of Aerospace Engineering, Middle East Technical University, 06531, Ankara, Turkey
yyaman@metu.edu.tr

Tarkan Çalışkan
Department of Aerospace Engineering, Middle East Technical University, 06531, Ankara, Turkey
tarkan@ae.metu.edu.tr

Volkan Nalbantoğlu
ASELSAN Electronics Industries, Akyurt, 06011, Ankara, Turkey
vnalbant@mgeo.aselsan.com.tr

Eswar Prasad
Sensor Technology Limited P. O. Box 97, Stewart Road, Collingwood, Ontario, Canada L9Y3Z4
eprasad@sensortech.ca

David Waechter
Sensor Technology Limited P. O. Box 97, Stewart Road, Collingwood, Ontario, Canada L9Y3Z4
dwaechter@sensortech.ca

Keywords: Smart structures, active vibration control, robust performance

Abstract

Theoretical and experimental results of the modeling of a smart plate is presented for active vibration control. The smart plate consists of a rectangular aluminum plate modeled in cantilever configuration with surface bonded piezoelectric patches. The patches are symmetrically bonded on top and bottom surfaces. The study uses ANSYS® (v.5.6) software to derive the finite element model of the smart plate. By using this model, the study first gives the influences of the actuator placement and size on the response of the smart plate and determines the maximum admissible piezoelectric actuation voltage. Based on this model, the optimal sensor locations are found and actual smart plate is produced. The experimental results of that smart plate are then used in the determination of a single input single output system model. By using this model, a single-input/single-output H_∞ controller is designed to suppress the vibrations due to the first two flexural modes of the smart plate. It has been shown that the designed controller guaranties robust performance.

Nomenclature

$\| \ \|_\infty$	Infinity norm of a signal or system
$\bar{\sigma}(M)$	Maximum singular value of matrix M
Δ	Norm bounded uncertainty block
F_l	Lower linear fractional transformation form
μ	Structured singular values for a system

Other parameters are clearly defined wherever applicable.

1 Introduction

The developments in the field of piezoelectric materials have motivated many researchers to work in the field of smart structures. A smart structure can be defined as a structure that can sense an external disturbance and respond to that with active control in real time to maintain the mission requirements. Smart structures consist of highly distributed active devices and processor networks. The active devices are primarily sensors and actuators either embedded or attached to an existing passive structure.

Bailey and Hubbard [1] initiated the research on the application of the smart structures in active vibration control. The utilization of discrete piezoelectric actuators has been shown to be a viable concept for vibration suppression of one dimensional structures by

Crawley and de Luis [2]. The vibration excitation of thin, flat plates by using piezoelectric patches has been analyzed by Dimitridis and Fuller [3].

The application of the finite element modeling techniques in the smart materials technologies has been in continuous growth during the last decade. Hence some piezoelectric elements have become available in commercial finite element codes like ANSYS®.

Wang [4] worked on the effectiveness of the finite element code ANSYS® in the modeling of the smart structures. In this work, the finite element method was proven to be a very effective tool for the analysis of the smart structures. Unlike the analytical techniques, the method offers fully coupled thermo-mechanical-electrical analysis of the smart structures. This allows the prediction of the reciprocal relations between the sensors and actuators. This allowance makes the development of the closed loop controller for active vibration control possible [5].

Using the time-delay techniques, Kalaycıoğlu [6], showed the effectiveness of the smart materials on the active control of space structures.

In one of the recent studies, Suleman *et al.* [7] proposed the effectiveness of the piezoceramic sensor and actuators on the suppression of vibrations on an experimental wing due to the gust loading. They showed the feasibility of the application of the smart structures in the suppression of vibrations due to the gust loading on the smart wing.

By using ANSYS®, Yaman *et al.* [8] worked on the finite element modeling technique for a smart beam. Based on their finite element model, they designed a controller that effectively suppressed the vibrations of the beam due to its first two modes. They demonstrated the effectiveness of H_∞ design technique and also evaluated the robust performance.

At the initial stages of the design, the finite element model is sufficient. The finite element modeling allows the determination of the optimal actuator and sensor placement, actuator size and power requirements. Generally, finite element method accurately predicts the natural frequencies and mode shapes of the structure. Since the technique makes no damping predictions, the transfer functions relating the inputs and the outputs of the systems are not usually very accurately determined.

Because of the difficulties in the development of an accurate finite element model of the smart structure, the technique is generally considered at the design stage. For the controller design, usually an experimentally identified model is used.

This study presents an active vibration control technique applied to a smart plate, which is composed of an aluminum flat plate modeled in cantilever configuration and with surface bonded piezoelectric patches (PZT). By using the experimentally identified model an H_∞ controller, that aims to suppress vibrations of the smart plate due to its first two flexural modes, is designed. The effectiveness of the technique in the modeling of the uncertainties is also presented.

2 Finite Element Modeling of the Smart Plate

In the theoretical analysis, finite element code ANSYS® (v5.6) was used. During the development of the smart plate, a model with parametric design capability is created.

The most suitable element having piezoelectric capability in three-dimensional coupled field problems is the solid type element SOLID5. Similar to other structural solid elements, this element has three displacement degrees of freedom per node. In addition to these degrees of freedom, the element has also potential degrees of freedom for the analysis of the electromechanical coupling problems [9]. Piezoceramic actuators inherently exhibit anisotropy and yield three-dimensional spatial variation in their response to electrical and mechanical stresses. Therefore, the models developed for the passive portion should include consistent degrees of freedoms with the actuator degrees of freedom at the locations where these elements interface.

Theoretically, the plate elements (shell or solid) can be used in the modeling of the passive portion of the smart structure. While the shell elements can be used in accordance with the thin plate theory, the solid elements work with the three dimensional elasticity theories. Hence, the utilization of solid type elements in the modeling of the passive portion allows the calculation of the effects of the normal stresses and the transverse shear stresses which may be developed in the passive portion of the smart structures.

Yaman *et. al*., [8] investigated the influences of the element type selection on the response of the smart structures. In their work, it was shown that the use of shell elements in the modeling of the passive portion leads to the inaccurate calculation of the global stiffness matrix. The modeling of the passive portion using consistent solid elements with the actuator elements however, is determined to yield accurate results.

In this work, solid elements (SOLID5) are used for the modeling of the active portion (piezoelectric actuators) and the compatible solid elements (SOLID45) are used for the passive portion (aluminum plate).

2.1 Effects of Actuator Placement

The influence of the placement of 24×(25×25×0.5 mm) patch actuators, made from BM500 piezoelectric material, on the aluminum plate is considered. The anisotropic material, piezoelectric and dielectric properties of BM500 type actuators are described by the piezoceramic manufacturer, Sensor Technology Limited [10]. By using modal analysis, the actuators are placed on the aluminum plate. In this work, the identically polarized patches are assumed to be bonded symmetrically on both top and bottom surface of the plate. The smart plate is considered to be clamped along one edge. The finite element model developed in the study is given in Figure 1.

Figure 2 shows the theoretical static response of the smart plate to piezoelectric actuation voltage. The first theoretically determined natural frequency and mode shape of the smart plate are shown in Figure 3

In order to determine the influences of the actuator placement on the response, two cases are considered. At each one, by keeping the distance between the piezoelectric patches constant, the x or y position of all actuators are varied from their original configurations, and the results are given in Figure 4. It is evident from the Figure 4 that as the patches are moved closer to the root (y=0) in y direction, the response increases. This is due to the higher strain developed near the root. For this reason, the patches should be placed on the plate as close as possible to the root. Furthermore, as the patches are moved closer to the (x=0) edge the response remains almost unaffected.

The influences of the actuator placement on the first mode is also investigated and the results are shown in Figure 5. It is again found that y-wise movement has greater effect.

2.2 The influences of the Actuator Size on the Response

Depending on the mission requirements, the size of the piezoelectric actuators can be altered. The effects of the increase in size of the actuator on the response are investigated in terms of the change in the coverage ratio. The coverage ratio is defined as the ratio of the area of the plate covered by the piezoelectric actuators to the total area. Using the original configuration of the smart plate, the coverage ratio is increased and the results for the piezoelectric actuation of 300V are shown in Figure 6. Although the increase in the length of the actuators makes smart plate stiffer, it also increases the energy transmitted to the smart plate giving rise to the response for the specified piezoelectric actuation value.

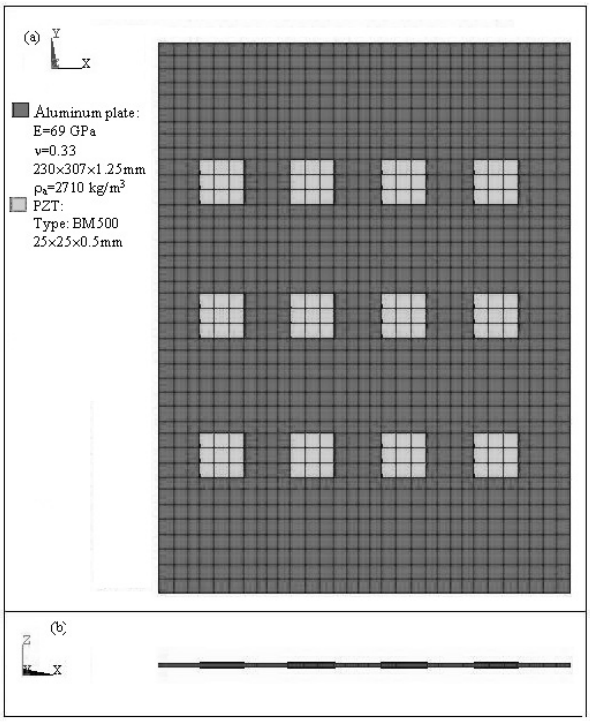

Figure 1. The geometry and the finite element model of the smart plate developed in the study
1.a. Top view
1.b. Side view

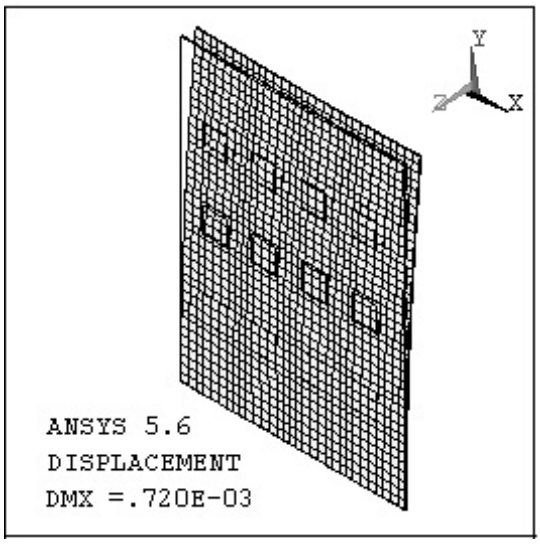

Figure 2. The theoretical response of the smart plate to a piezoelectric actuation of 300V

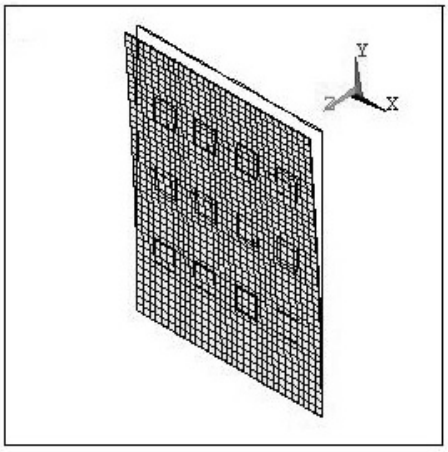

Figure 3. The first theoretical mode shape of the smart plate (f_1=11.625 Hz)

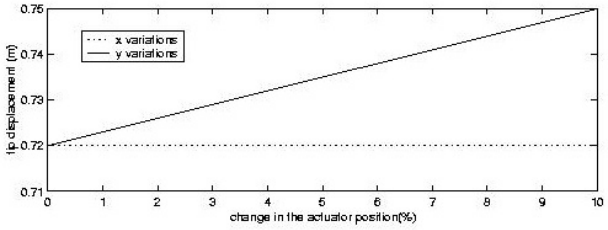

Figure 4. The influences of the actuator placement on the response at 300V

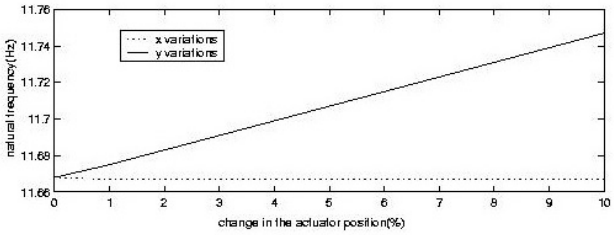

Figure 5. The influences of the actuator placement on the first theoretical natural frequency of the smart beam

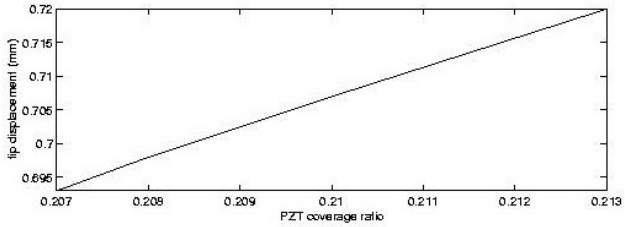

Figure 6. The influence of the actuator size variation on the response of the smart plate

2.3 The Influence of the Transverse Stresses and the Normal Stresses

The modeling of the passive portion by using the compatible solid elements not only guaranties the proper transfer of the generated nodal forces on the passive elements, but also allows the computation of the transverse shear and normal stresses developed on the passive portion of the smart plate due to the piezoelectric actuation.

In order to investigate the importance of these transverse stresses, the maximum stresses developed on the passive portion of the smart plate by the piezoelectric actuation is calculated. Figure 7 gives the variation of the stress components as a function of the piezoelectric actuation voltage. It can be seen that the transverse normal and shear stresses, are not zero. Therefore, the exclusion of these stresses, hence using shell elements, may lead to inaccurate results

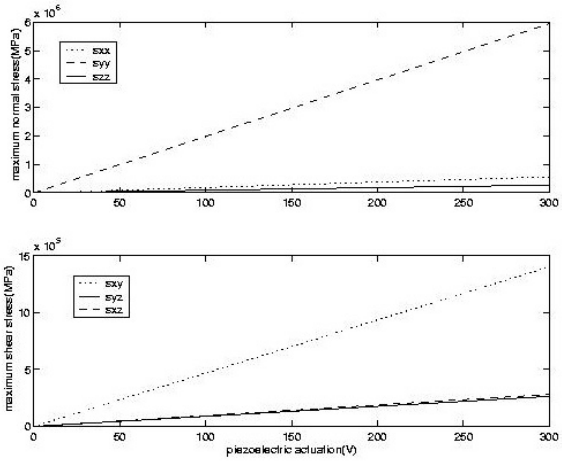

Figure 7. The comparison of the maximum normal and shear stresses developed on the passive portion of the smart plate due to the piezoelectric actuation (s_{xx}, s_{yy}, s_{zz} are the maximum normal stress components along x, y and z directions respectively)

2.4 The Maximum Admissible Piezoelectric Actuation

Piezoelectric materials are brittle and have tensile strengths in the order of 63 MPa. Therefore, the stress in the actuators can be critical in adverse applications. In order to determine the maximum possible piezoelectric actuation value, the Von Mises stresses developed in the actuators should be investigated prior to the operation. For this reason, Von Mises stresses for various actuation voltages are calculated and results are shown in Figure 8. Since the resultant Von Mises stresses are in the order of 1 MPa, for normal operating conditions (200-300V) the piezoelectric actuators are not expected to fail.

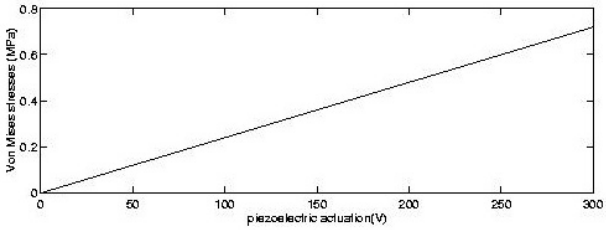

Figure 8. The effect of the piezoelectric actuation voltage on the Von Mises stresses developed within the piezoelectric actuators.

2.5 Placement of Strain Gages

Finite element method also allows the determination of the most suitable locations of the sensors for active vibration control. These locations can be determined by the utilization of the mode shapes of the smart structure. In this work, by using the modal analysis results of the smart plate, three locations are determined for the strain gage sensors to sense vibrations of the smart plate. The optimum locations so obtained and the configuration of the strain gages and the piezoelectric sensors on the smart plate are shown in Figure 9. In this model, while the strain gage at location (1) is used for the measurement of strain in x direction, locations (2) and (3) are considered in the measurement of the strain in y direction. By using the initial configuration of the smart plate, the response of the smart plate to various actuation values are calculated. Figure 10 gives the response of the smart plate in terms of the strain at these measurement locations. It can be seen from this figure that the location (2) gives the highest response.

Since the theoretical model is in the linear range of the elasticity and piezoelectricity, the

response is accordingly found to vary linearly with the actuation voltage

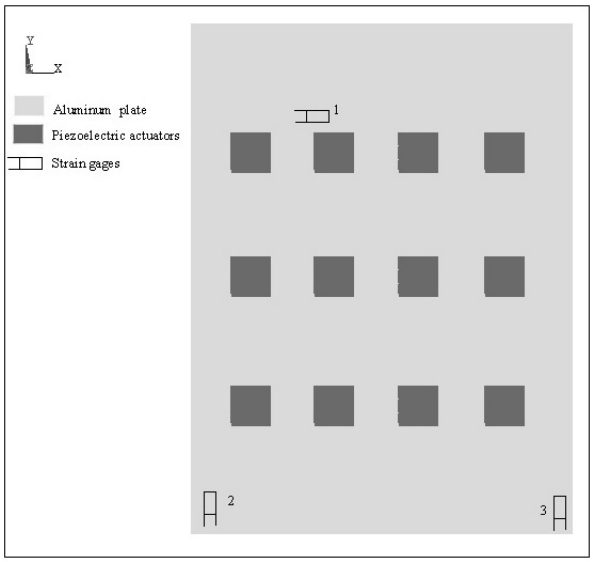

Figure 9. The placement and the configuration of the strain gages and piezoelectric patches on the smart plate

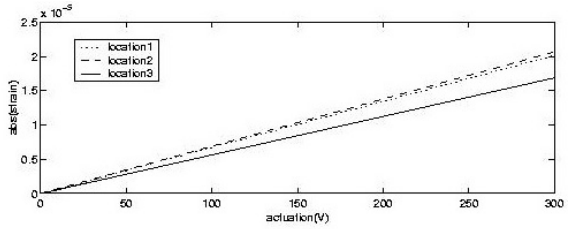

Figure 10. The comparison of the variation of the piezoelectric actuation on the response of the smart plate (location (1): ε_x, locations (2) and (3): ε_y)

3 The Test Article

By using the results obtained from the theoretical analysis of the smart plate, the test article was produced.

During the development of the test article thin glass-epoxy patches are placed between the piezoelectric actuators and the aluminum plate. The placement of the insulating layers not only allows the individual actuation of piezoelectric patches but also makes the utilization of the piezoelectric actuators possible as the collocated sensor and actuator pairs, without creating a short circuit.

The test article was produced and tested at Sensor Technology Limited of Canada. The smart plate model consists of 24 × (25×25×5 mm) symmetrically placed BM500 type piezoelectric actuators and 24× (38×38×0.165mm) glass epoxy insulating layers. It further contains 6 symmetrically placed SG-7 LY13 type strain gages (Omega Engineering, CT) to sense the bending vibrations. The test article is shown in Figure 11.

In the current study, as a result of the analysis explained in Section 2, only the strain gage sensor pair labeled (2) are used in the extraction of the experimental transfer functions.

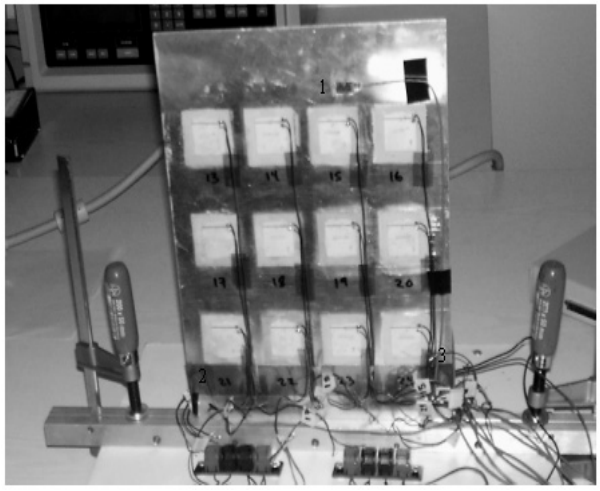

Figure 11. The test article used in the study

Table 1 gives the comparison of the theoretical and experimental results. It can be seen from the table that the presence of the thin insulating layer influences the second resonance frequency of the smart plate most.

Frequency (Hz)	FEM	Experimental
f_1	11.63	11.88
f_2	37.86	41.47
f_3	73.24	71.62

Table 1. The comparison of the theoretical and experimental resonance frequencies of the smart plate. (f_1: First flexural mode, f_2: First torsional mode, f_3: Second flexural mode)

4 System Identification

An accurate model of the input/output behavior of the system is required for controller design. One way to achieve this is the utilization of the finite element modeling technique. However, due to the difficulties in the determination of an accurate finite element model for the smart plate, this technique is considered to be less effective compared to the system identification technique [11]. In the system identification technique, the most convenient system model to be used in the controller design is obtained by curve fitting a transfer function model to the experimental frequency response function [12]. The application of this technique results in a 14^{th} order transfer functions from the actuators to the sensor at the location (2). The comparisons of these models with the experimental transfer function is shown in Figure 12. This 14^{th} order model does not capture the modes above 1100 rad/sec. These unmodeled modes will be treated as uncertainties in the control design.

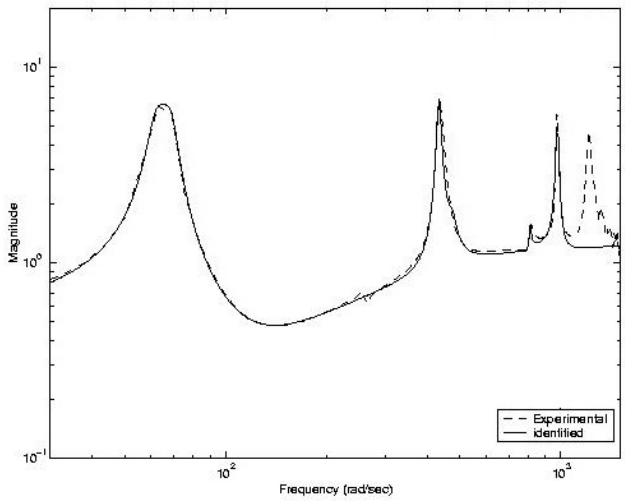

Figure 12. The comparison of the experimental and identified models

5 H_∞ Controller Design

Based on the model obtained in Section 4, an H_∞ controller is designed for the smart plate. The goal of the controller is to attenuate the vibrations of the smart plate at its first two flexural frequencies (in the range from zero to 600 rad/sec) and gain stabilize the unmodeled high frequency modes.

In H_∞ control design framework, the objective is to minimize the H_∞ norm of the weighted transfer functions from the input disturbance signals to the output error signals, [15,16]. The uncertainties in the plant model can be put in such a form that some of the disturbances and error signals correspond to the channels through which the nominal model interacts with a norm bounded uncertainty block Δ. This generates the set of plants in which the true plant is assumed to exist. This framework is represented in Figure 13.

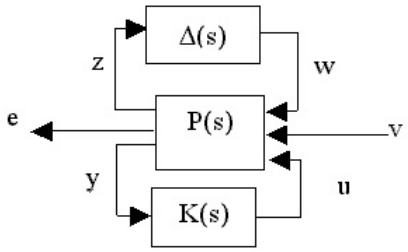

Figure 13. The modeling of uncertainties

Here, P is the nominal plant model with appropriate weights to reflect the design goals, K is the controller to be designed, and Δ is the norm bounded uncertainty block, v is a vector of exogenous inputs such as reference commands, disturbances and noise, e is a vector of error signals to be kept small, y is a vector of sensor measurements and u is a vector of control signals, w and z are the disturbance and error channels corresponding to the uncertainty block Δ respectively.

For the design purposes, the Δ block is eliminated and the input-output map from $[w\ v]^T$ to $[z\ e]^T$ is expressed in lower linear fractional transformation form $F_l(P, K)$ as

$$\begin{bmatrix} z \\ e \end{bmatrix} = F_l(P,K) \begin{bmatrix} w \\ v \end{bmatrix} \qquad (1)$$

where, $F_l(P, K) = P_{11} + P_{12}K(I - P_{22}K)^{-1}P_{21}$

Assuming that plant P is partitioned according to the dimensions of the control, measurement, disturbance and error signals, as

$$P = \begin{bmatrix} P_{11} & P_{12} \\ P_{21} & P_{22} \end{bmatrix} \quad (2)$$

The objective is to find a stabilizing controller K that minimizes the ∞-norm of $|| F_l (P, K) ||_\infty$. For an uncertainty block *satisfying* $|| \Delta ||_\infty < 1$ the closed loop system in Figure 14 has robust performance *if* $|| F_l (P, K) ||_\infty \leq 1$ is achieved [16].

This result, however, is conservative because it assumes that the delta block is a full block with no structure to it. The uncertainties in a realistic problem are due to the components of a system, and representation of such uncertainties results in a block diagonal Δ. A less conservative robustness test for the closed loop system is given by examining the structured singular values (μ) of $M = F_l (P, K)$. For a given system M and an uncertainty structure, the structured singular value μ is defined as [14].

$$\mu_\Delta = \frac{1}{min\{\bar{\sigma}(\Delta) : \Delta \in \Delta', det(I - M\Delta) = 0\}} \quad (3)$$

where Δ′ is the set of block diagonal matrices with a structure defined by the problem formulation. If no Δ∈Δ’ makes *(I-MΔ)* singular then $\mu_\Delta(M)=0$

For an appropriately weighted control design formulation, a μ value of less than one across all frequencies indicates robust performance.

The H_∞ controller synthesis and μ-analysis techniques described above are applied to the smart plate.

In H_∞ controller design for the smart plate, the performance objective is to minimize the maximum frequency response of the first two flexural modes of the smart plate at the sensor locations. Figure 14 shows the formulation of the closed loop control in H_∞ framework.

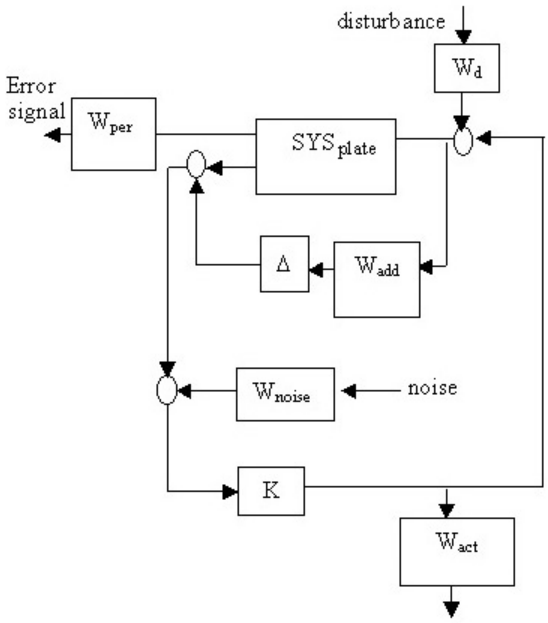

Figure 14. The block diagram formulation of the control problem

In Figure 14, SYS_{plate} defines the nominal smart plate model, W_{per} represents a performance weight on the strain gage sensor to achieve the performance objective. The W_{per} weight is shown in Figure 15. This weight is selected to achieve attenuation in the peak frequency response of the closed-loop system.

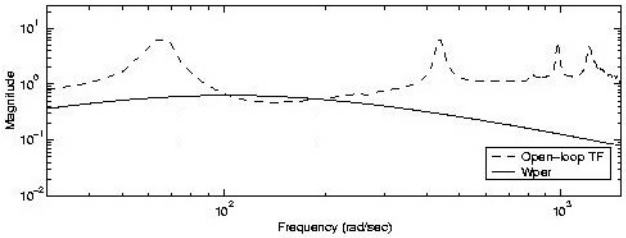

Figure 15. The comparison of the performance weight W_{per} and the experimental transfer function at the strain gage location (2)

An additive uncertainty is included in the problem formulation to account for the unmodeled high frequency modes and modeling errors inside the controller bandwidth. This weight is selected to have a magnitude greater than the structural modes above 600 rad/sec. If robust stability of the closed-loop system is achieved for this additive uncertainty model, the

flexible modes of the structure will be gain stabilized above 600 rad/sec. Figure 16 shows the magnitude of W_{add} versus the magnitude plot of the transfer function from the piezoelectric actuators to the strain gage sensors.

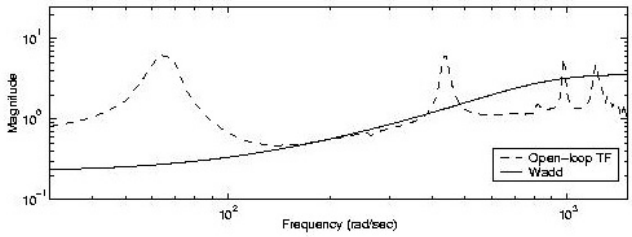

Figure 16. The comparison of the additive weight W_{add} and the experimental transfer function at the location (2).

To limit the actuator command signal in the control design process to 250 volts W_{act} in Figure 16 is chosen as 1/250. The weight on the disturbance input, W_{dist} is taken to be 1. This indicates that the input disturbance is expected to be on the same order of magnitude as the controller signals. The strain gage signal has a signal to noise ratio of 100. Therefore, W_{noise} in Figure 13 is taken as 0.01. A 19^{th} order controller is obtained by applying the standard solution techniques to the system formulated in Figure 13. This controller is tested on an 18^{th} order model of the smart plate (capturing the modes of the system up to 1600 rad/sec) obtained from the experimental data by using system identification as explained in Section 4. Open and closed loop frequency response of the system is shown in Figure 17. The comparison of the time domain responses are shown in Figure 18.

Figure 19 gives the μ- analysis results. A maximum μ value of approximately one indicates that the robust performance requirements are satisfied for the closed loop system

The attenuation levels (open loop/closed loop peak values) of 6/1 and 2.2/1 are achieved for the first and the second flexural modes respectively.

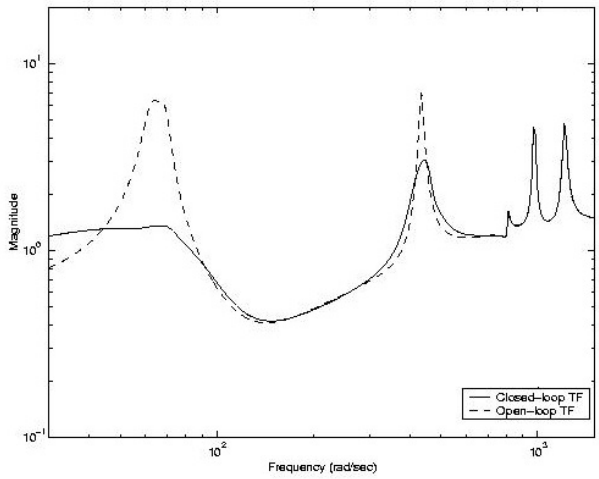

Figure 17. The comparison of the open and closed loop responses of the smart plate

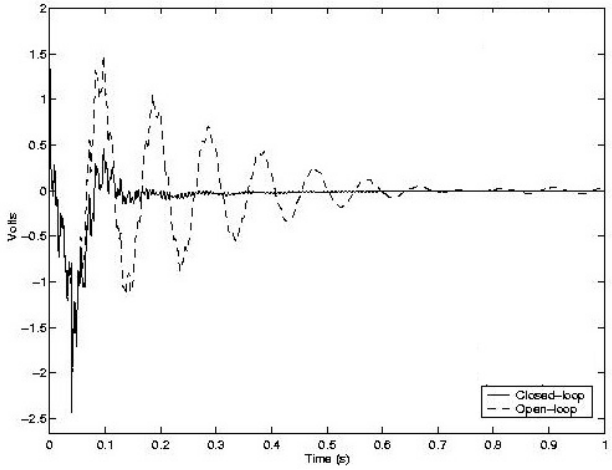

Figure 18. The comparison of the open and closed loop responses to a step input

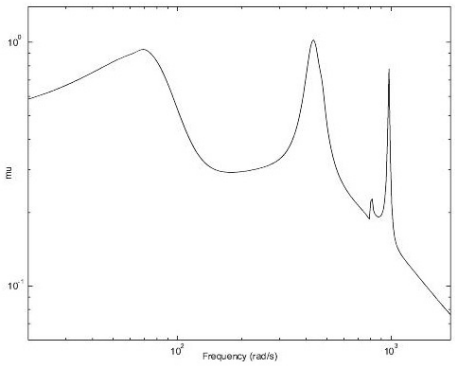

Figure 19. The structural singular value (μ) of the closed loop system

5 Conclusions

This study presented an H_∞ active vibration control technique applied to a smart plate. Based on the finite element modeling technique, the study first analyzed the problems in the determination of the placement and size of the PZT actuators and the placement of the strain gage sensor. Hence an optimum number and locations for PZT actuators and the optimum locations for the strain gage sensors were determined.

Because of the difficulties in the development of an accurate finite element model of the smart plate, an experimentally identified model of the smart plate was utilized in the design of the H_∞ controller. The designed controller was found to suppress the in-vacuo vibrations of the smart plate due to its first two flexural modes. It was also shown that the designed controller guarantied the robust performance of the system in the presence of uncertainties.

Acknowledgements

This work was supported by NATO/RTO/Applied Vehicle Technology Panel through the project T-121 'Application of Smart Materials in the Vibration Control of Aeronautical Structures'. The authors gratefully acknowledge the support given.

References

[1] Bailey, T. Hubbart, J. E. 1985, Distributed Piezoelectric-Polymer Active Vibration Control of a Cantilever Beam. *Journal of Guidance, Control and Dynamics*, Vol.8, No. 5, pp 605-611.

[2] E. F. Crawley, J. Louis, Use of Piezoelectric Actuators as Elements of Intelligent Structures. *AIAA Journal*, October 1989.

[3] E. K. Dimitridis C., R. Fuller, C. A. Rogers Piezoelectric Actuators for Distributed Vibration excitation of Thin Plates, *Journal of Vibration and Acoustics*, vol. 113, pp. 100-107, Jan. 1991

[4] Wang and C. K. Jen, Design and Fabrication of Composites for Static Shape Control. *Final Report NRC-CNRC*, 1996

[5] S. E. Prasad, J.B. Wallace, B. E. Petit, H. Wang C.K. Jen. Kalaycioglu, M. Giray Development of Composite Structures for Static Shape Control. *SPIE, Far East and Pacific Rim Symposium on Smart Materials, Structures and MEMS*. (Bangor, India)

[6] S. Kalaycıoğlu, M. M. Giray and H. Asmer, Time Delay Control of Space Structures Using Embedded Piezoelectric Actuators and Fiber optic Sensors. SP*IE's 4th Annual Symposium on Smart Structures, and Materials,* March 1997.

[7] A. Suleman, A. P. Costa, C. Crawford, R. Sedaghati, Wind Tunnel Aeroelastic Response of Piezoelectric and Aileron Controlled 3-D Wing. *CanSmart Workshop SmartMaterials and Structures,* Proceedings, Sep. 1998

[8] Y. Yaman, T. Çalışkan, V. Nalbantoğlu, D. Waechter, E. Prasad, Active Vibration Control of a Smart Beam. Canada-US *CanSmart Workshop Smart Materials and Structures* proceedings, Oct. 2001 Montreal Quebec, Canada

[9] ANSYS® User's Manual (version 5.6), *ANSYS Inc.Southpointe 275 Technology Drive Canonsburg, PA, 15317.*

[10] Sensor Technology Ltd. *Product Data Sheets*, www.SensorTech.ca, 2001

[11] J. Dosch, J. Inmann, Modeling and Control for Vibration Suppression of a Flexible Active Structure. *Journal of Guidance, Control and Dynamics*, Vol. 8, April, 1995

[12] V. Nalbantoğlu, *Ph.D. Thesis*, University of Minnesota, 1998, Robust Control and System Identification for flexible structures

[13] K. Zhou, J.C. Doyle, K. Glove *Robust and OptimalControl*. Prentice Hall, New Jersey, 1996

14] G. Balas, J. Doyle, K. Glover, A. Packard, *Matlab®(v.6.0) μ-Toolbox Users's Manual*

[15] J. Doyle , B. Francis and A. Tanenbaum, *Feedback Control Theory*, Mac Millan Publishing, New York,1992